Available online at www.sciencedirect.com
SCIENCE DIRECT®
Biochemical Pharmacology 68 (2004) 1465–1475
Biochemical Pharmacology
www.elsevier.com/locate/biochempharm

Evaluation of glutathione deficiency in rat livers by microarray analysis

Naoki Kiyosawa*, Kazumi Ito, Kyoko Sakuma, Noriyo Niino, Miyuki Kanbori, Takashi Yamoto, Sunao Manabe, Naochika Matsunuma

Medicinal Safety Research Labs., Sankyo Co. Ltd., 717 Horikoshi, Fukuroi, Shizuoka 437-0065, Japan

Received 20 April 2004; accepted 27 May 2004

Abstract

Hepatic glutathione content was measured and gene expression data were obtained using an Affymetrix RG U34 array after treatment with tap water containing 20 mM L-buthionine (*S, R*)-sulfoximine (BSO) to male F344 rats for four consecutive days. Both Spearman's and Pearson's correlation coefficients were calculated between the glutathione content and the mRNA content level obtained from the microarray analysis individually. Sixty-nine gene probes, which were statistically significant (Spearman's correlation, $P < 0.05$) and showed a Pearson's correlation coefficients (Pearson's r) less than -0.8 between mRNA content and hepatic glutathione content, were identified as glutathione deficiency-correlated probes. By comparing the hepatic gene expression profiles between BSO- and butylated hydroxyanisole (BHA)-treated rats, 14 probes of genes that showed an increase in the corresponding gene mRNA levels only after the BSO treatment were thought to be good indicators of glutathione deficiency. A principal component analysis successfully illustrated the time-course of hepatic gene expression after the treatment with acetaminophen, phenobarbital and clofibrate, and the expression profiles were thought to reflect the changes in hepatic glutathione levels. The identified gene probes in the present study would be useful as markers for assessing hepatocellular glutathione deficiency, or oxidative stress level, based on microarray data.

Keywords: Glutathione; L-buthionine (*S, R*)-sulfoximine; Butylated hydroxyanisole; Acetaminophen; Liver; Microarray

1. Introduction

Hepatotoxicity is one of the major causes of drug withdrawal from the market [1]. Although many of the clinical hepatotoxicity events cannot be predicted in the preclinical trials, some mechanisms of hepatotoxicity caused by drug treatment have been well investigated. Acetaminophen (APAP) and carbon tetrachloride are representative hepatocyte necrotic compounds, and a hepatic glutathione depletion precedes the onset of necrosis [2]. Glutathione serves vital functions in detoxifying electrophiles and scavenging free radicals [3]. Stimulation of glutathione synthesis and induction of phase II drug metabolizing enzymes (DMEs) including glutathione *S*-transferase (GST) protect cells from oxidative stress by conjugating or scavenging the oxidative electrophile molecules or reactive oxygen species [4]. In the case of APAP overdosing, APAP is metabolically activated by phase I DME to form a reactive metabolite *N*-acetyl-*p*-benzoquinone imine (NAPQI), which covalently binds to protein [5,6]. Although NAPQI is detoxified by glutathione conjugation, an excess dose of APAP depletes 90% of the hepatic glutathione, and the reactive NAPQI forms protein adducts [6,7]. Thus, the potential glutathione depletory risk caused by the treatment of developing drugs should be carefully assessed in the preclinical studies, and efficient methods for evaluating the cellular glutathione level should be developed for assessing the potential risk of APAP-type hepatic injury or perturbation of hepatocellular glutathione homeostasis.

Under the oxidative stress conditions, phase II DME and antioxidant genes play a central role in eliminating reactive oxygen species or electrophilic metabolites generated from chemical oxidation by the phase I DMEs [8]. Transcriptional induction of phase II DME genes is known to be

Abbreviations: APAP, acetaminophen; ARE, antioxidant response element; BHA, butylated hydroxyanisole; BSO, L-buthionine (*S, R*)-sulfoximine; CAR, constitutive androstane receptor; CLO, clofibrate; CYP, cytochrome P450; DME, drug metabolizing enzyme; γ-GCS, γ-glutamylcysteine synthetase; GST, glutathione *S*-transferase; NAPQI, *N*-acetyl-*p*-benzoquinone imine; Nrf2, NF-E2-related factor-2; Pearson's *r*, Pearson's correlation coefficient; PB, phenobarbital; PCA, principal component analysis

* Corresponding author. Tel.: +81-538-42-4356; fax: +81-538-42-4350.
E-mail address: kiyosawa@sankyo.co.jp (N. Kiyosawa).

0006-2952/$ – see front matter © 2004 Elsevier Inc. All rights reserved.
doi:10.1016/j.bcp.2004.05.053

mediated by two different mechanisms: receptor-mediated and non-receptor-mediated pathways [9]. The receptor-mediated pathway is stimulated by nuclear receptors such as the aryl hydrocarbon receptor (AhR), constitutive androstane receptor (CAR) or pregnane X receptor (PXR) [9–11], while the non-receptor-mediated pathway is regulated by NF-E2-related factor-2 (Nrf2), a basic leucine zipper transcription factor [12–14]. Under oxidative stress, Nrf2 translocates to the nucleus after dissociation from INrf2 [15]. Then, Nrf2 in the nucleus binds to the antioxidant response element (ARE) sequences, leading to the transcriptional induction of target genes such as GSTα [16], heme oxygenase-1 [17], or γ-glutamylcysteine synthetase (γ-GCS), which is a rate-limiting enzyme for glutathione synthesis [18]. These favorable reactions including improved glutathione availability render cells to be protected against cellular oxidative stress.

L-buthionine (*S, R*)-sulfoximine (BSO) is a specific inhibitor of γ-glutamylcysteine synthetase (γ-GCS), and, consequently, inhibits glutathione synthesis [19]. This chemical is useful for generating a glutathione-deficient animal model [20]. Butylated hydroxyanisole (BHA) is a phenolic antioxidant and induces the transcription of many phase II DME and antioxidant genes via the Nrf2-mediated pathway [21], irrespective of the cellular redox status. In the present study, we identified a set of marker genes by microarray analysis for the evaluation of hepatocellular glutathione levels in glutathione-deficient rats treated with BSO. In addition, we performed a microarray analysis on rat livers treated with BHA. The gene expression profiles between BSO- and BHA-treated rat livers were compared, and the inductive manner of phase II DME or antioxidant genes was investigated. Finally, we present a reasonable procedure for analyzing the two different induction mechanisms of phase II gene expression, namely, a receptor-mediated and non-receptor-mediated induction pathway, by considering the change in mRNA contents of nuclear receptor target genes or antioxidant genes.

2. Materials and methods

2.1. Materials and animal treatment

BSO, BHA, APAP, phenobarbital (PB) and clofibrate (CLO) were purchased from Sigma–Aldrich. Eight-week-old male F344/DuCrj rats were purchased from Charles River Inc., Japan and nine-week-old animals were used in this study. Animals were maintained in a room controlled at a temperature and relative humidity of 24 ± 2 °C and 40–70%, respectively, and given food and water ad libitum. Animal groups consisting of four rats were administered BHA by gavage at a dose of 0.8% (w/w) or tap water containing 20 mM of BSO, for four consecutive days, and were euthanized under ether anesthesia at the end of the study. Animal groups consisting of four rats were orally administered APAP (1000 mg/kg) or distilled water, and were euthanized under ether anesthesia at 1, 2, 6 or 24 h, after the dosing. Animal groups consisting of four rats were orally administered with PB (100 mg/kg body weight per day) or CLO (200 mg/kg body weight per day) or the corresponding vehicles (water for PB and 1% Tween-80 for CLO), once daily during the experimental period, and were euthanized under ether anesthesia 24 h after the 1st, 4th and 14th dosings of PB (referred to as day 1, day 4 and day 14, respectively), 24 h after the 1st, 4th and 7th dosings of CLO (day 1, day 2 and day 4, respectively). After the euthanasia, the left lateral lobes of the livers were removed and stored at −80 °C until use. The experimental protocol was approved by the Ethics Review Committee for Animal Experimentation of Sankyo Co. Ltd.

2.2. Measurement of glutathione contents

The liver samples (0.1 g) were homogenized with 5% 5-sulfosalicylic acid (Sigma–Aldrich), and centrifuged at 12,000 rpm for 10 min at 4 °C. The supernatant was used for the measurement of total glutathione content in the liver using Total Glutathione Quantification Kit (Dojindo Laboratories) according to the manufacturer's instructions.

2.3. Microarray analysis

Liver samples were homogenized with the RLT buffer supplied in the RNeasy Mini Kit (QIAGEN Inc.), and total RNA was isolated according to the manufacturer's instructions. Microarray analysis was performed according to the Affymetrix standard protocol. Briefly, a total RNA of 5 μg prepared from the individual rat liver samples was used for cDNA synthesis using a T7-$(dT)_{24}$ primer (Amersham Biosciences). A biotin-labeled cRNA mix was transcribed using BioArray High Yield RNA Transcription Labeling Kit (Enzo Diagnostics). Every biotin-labeled cRNA target sample (approximately 10 μg) was individually hybridized to a Rat Genome U34A Array (Affymetrix Inc.), which contains a total number of 8799 probe sets, at 45 °C for 16 h. GeneChip® was washed and stained using Fluidics Station (Affymetrix Inc.) and scanned with a GeneArray® Scanner (Affymetrix Inc.). Microarray image data obtained from rat livers were analyzed with Microarray Suite version 5.0 (Affymetrix Inc.). The numerical data were normalized by the trimmed-mean normalization method, where the global mean was normalized after trimming the top 2% and bottom 2% of the GeneChip data [22]. Furthermore, *z*-score normalization was conducted for the global mean normalized data [23].

2.4. Identification of glutathione deficiency-correlated gene probes

Both Spearman's and Pearson's correlation coefficients between the hepatic glutathione content and gene expres-

Table 1
Primer and probe sequences for real-time quantitative RT-PCR

Gene	Accession number	Primer/probe sequence
γ-GCS	S65555	Forward: TCGCCTACAAAAAGCGT CACT Reverse: CCAGGGAGGTACTTAAACTCAACAC Probe: AGGCGTGAATGTGGTGGTTTGGCA
Ferritin light-chain 2	AI231807	Forward: CTTGAGATGGCTTCTGCACATC Reverse: TCTCCTCAAGTTGCAGAACGAA Probe: TGGAAGAGTGCACGGCCCCC
GTP cyclohydrolase I	E03424	Forward: TGAACAGCAAGACTGTCACTAGCA Reverse: GAACTCCTCCCGAGTCTTTGG Probe: CATGCTAGGCGTGTTCCGGG
Glutathione reductase I	U73174	Forward: GGGATTGGCTGCGATGAG Reverse: GGTGGCCCCCATTTTCAC Probe: TGCTTCAGGGCTTCGCTGTAG

sion data obtained for each probe were calculated using Spotfire® and Microsoft® Excel [24,25]. Probes that gave presence calls for all the BSO-treated rats ($n = 4$) were used for analysis. In this study, we determined the glutathione deficiency-correlated probe sets (glutathione-deficiency probes) by identifying the probes that gave statistically significant results (Spearman's correlation, $P < 0.05$) and a Pearson's correlation coefficient (Pearson's r) of less than -0.8. A sequence homology search was performed for non-annotated probes using BLAST Homology Search [26]. Probes that did not show sequence homology to known genes were excluded from the study.

2.5. Comparison of gene expression profiles of BHA- and BSO-treated rat livers

Microarray data were normalized by the trimmed-mean normalization method. The fold change of a probe in both BHA- and BSO-treated rat livers was calculated by dividing the mean signal value of chemical-treated rats by that of the control rats. The set of probe genes for which the mRNA content was statistically different and mean fold-change between chemical-treated ($n = 4$) and control ($n = 4$) rats was above 1.5 (up-regulated genes) or below 0.66 (down-regulated genes) were determined, and used for the calculation of hierarchical clustering [27] (using Pearson's r as a distance measure) based on the microarray data obtained from the BSO-treated, BHA-treated and control rat livers after trimmed-mean normalization followed by z-score normalization.

2.6. Real-time quantitative RT-PCR analysis

Total RNA of 5 μg was treated with 5 U of DNase I (Takara) in the manufacturer's buffer containing 40 U of RNase inhibitor (TOYOBO) in a final volume of 50 μL, and subjected to phenol-chloroform purification. DNase I-treated total RNA of 2 μg was reverse-transcribed in the manufacturer's buffer supplemented with 10 mM of dithiothreitol, 0.5 mM of dNTPs, 200 U of Superscript II (Invitrogen) and 40 U of RNase inhibitor in a final volume of 20 μL. The gene sequences of γ-GCS (accession no. S65555), ferritin light-chain 2 (AI231807), GTP cyclohydrolase I (E03424) and glutathione reductase I (U73174) were downloaded from the NCBI database (http://www.ncbi.nlm.nih.gov/) according to the corresponding accession numbers. Real-time quantitative RT-PCR primers and probes were purchased from Nippon EGT. The primer and probe sequences are listed in Table 1. Quantitative RT-PCR was performed using the qPCR™ Mastermix Plus (Eurogentec), and the mRNA content level was quantified with a GeneAmp® 5700 Sequence Detection System (Applied Biosystems), according to the manufacturer's instruction. For internal control, Rodent GAPDH Control Kit (Applied Biosystems) was used.

2.7. Principal component analysis

Trimmed-mean normalized microarray data obtained from rat livers treated with BSO, BHA, APAP, PB and CLO were used for a principal component analysis (PCA). Spotfire was used for the calculation of PCA using gene expression data of glutathione-deficiency probes.

2.8. Statistical analysis

The glutathione content data were analyzed by the F-test to evaluate the homogeneity of variance. If the variance was homogeneous, Student's t-test was applied. If the variance was heterogeneous, Aspin–Welch's t-test was performed. A significance level of $P < 0.01$ or $P < 0.05$ was considered acceptable. Spearman's rank correlation between GeneChip and hepatic glutathione content data was calculated using Microsoft Excel, and a significance level of $P < 0.05$ was considered significant. Pearson's r between GeneChip and hepatic glutathione content data was calculated using Spotfire.

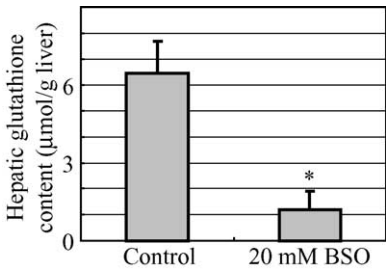

Fig. 1. Hepatic glutathione content. Hepatic glutathione content was measured after the 4-day treatment of 20 mM BSO mixed with tap water in rats. Data are represented as means ± S.D. of four rats. * Significantly different from the control group ($P < 0.01$).

3. Results

3.1. Glutathione contents in the BSO-treated rat liver

The mean glutathione content in rat livers treated with 20 mM of BSO was significantly decreased as compared to that of the control group ($P < 0.01$, Fig. 1). The glutathione mean content in the BSO-treated rat livers was 1.20 μmol/g liver, 0.19-fold that of the control group (6.48 μmol/g liver).

3.2. Identification of glutathione deficiency-correlated gene probes

There were 69 glutathione deficiency-correlated genes as determined by measuring their expression levels, which were statistically correlated with the hepatic glutathione content (Spearman's correlation, $P < 0.05$) and gave a Pearson's r below -0.8 (Table 2). Of all the probes in the RG U34 array, the probe for the GST Ya gene showed the highest inverse-correlation with the hepatic glutathione content.

3.3. Comparison of gene expression profiles in BHA- and BSO-treated rat livers

Hierarchical clustering was conducted for the microarray data obtained from the BSO-treated, BHA-treated rat and control rat livers, using the probe set consisting of both BSO- and BHA-selected probes (Fig. 2). Up-regulated genes were clearly classified into three patterns: BSO-specific, BHA-specific and dually up-regulated. On the other hand, down-regulated genes did not show clear patterns as compared to those of the up-regulated genes. As the hepatic mRNA content of 42 genes was increased by both the BSO and BHA treatments, these 42 genes were referred to as ''dually-induced gene probes'' (Fig. 3). The hepatic mRNA content of 32 and 43 gene probes satisfied the criteria for a BHA and BSO treatment-specific increase in gene expression, respectively (Figs. 4 and 5). BHA-specific probes identified many phase II DME genes such as GST and UDP-glucuronyltransferase

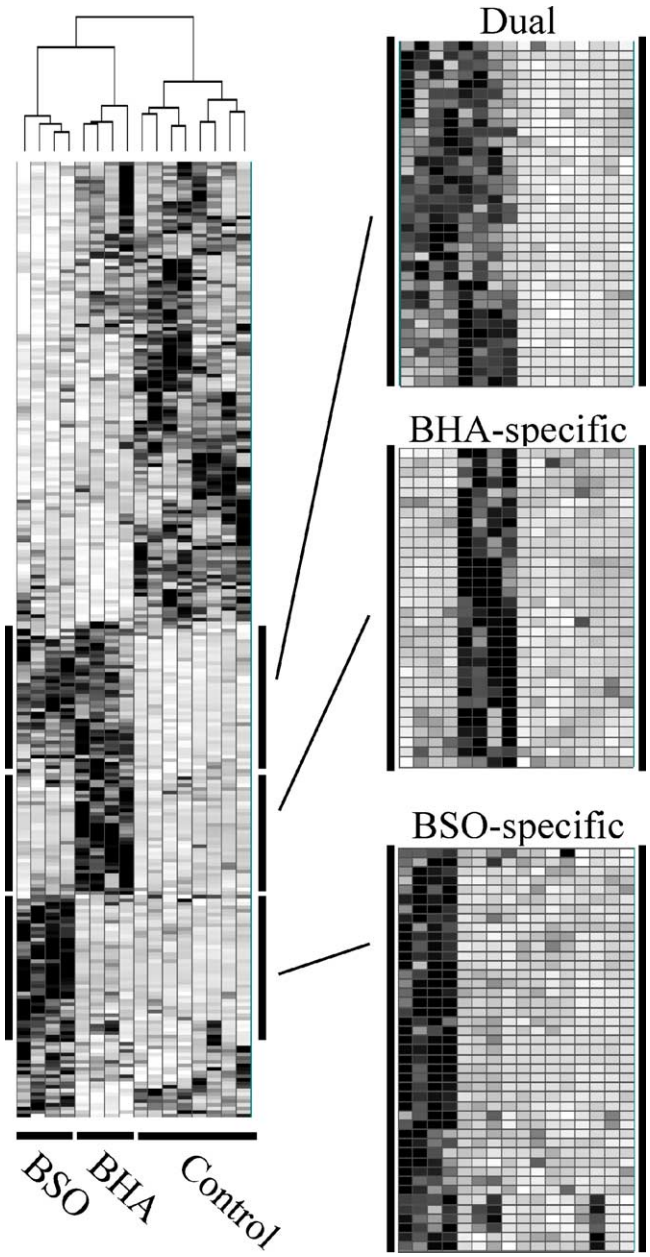

Fig. 2. Gene expression profiles of rat livers treated with BSO or BHA. Probe set of genes, which showed mRNA contents that were statistically different and mean fold ratios compared between the chemical-treated ($n = 4$) and control ($n = 4$) rats, that were above 1.5 (induced genes) or below 0.66 (repressed genes) was used for the calculation of hierarchical clustering based on the microarray data obtained from the BSO-treated, BHA-treated and control rat livers. The colors of the heat map represent the transcription levels: white for low, gray for intermediate and black for high transcription levels.

(UDPGT) family genes (Fig. 4). In addition, BHA-specific probes identified CAR target genes such as cytochrome P450b (*CYP2B*), Mrp3 and alcohol dehydrogenase. On the other hand, 17 probes identified genes induced specifically by BSO, including a number of antioxidant genes such as metallothionein, ferritin and thioredoxin reductase (Fig. 5). In addition, the γ-GCS light chain and glutathione reductase I, which are important for cellular glutathione

Table 2
Glutathione deficiency-correlated probes

Annotation	Affymetrix ID	Fold change	Pearson's *r*
Conjugation			
Glutathione *S*-transferase Ya subunit	K00136mRNA_at	2.21	−0.99
GST Ycl	X78848cds_f_at	2.29	−0.98
Bilirubin-specific UDP-glucuronosyltransferase	S56936_s_at	6.96	−0.93
UDP-glucuronosyltransferase (UGT2B12)	U06274_s_at	1.45	−0.91
Glutathione *S*-transferase Yc2 subunit	S82820mRNA_s_at	33.02	−0.91
Hydroxysteroid sulfotransferase a (STa)	M33329_f_at	1.53	−0.90
Glutathione *S*-transferase (GST) Y(b) subunit	X04229cds_s_at	1.41	−0.90
3-MC-inducible truncated UDP-glucuronosyltransferase	J05132_s_at	1.49	−0.88
Glutathione *S*-transferase Yc2 subunit	S72506_s_at	21.59	−0.88
Glutathione *S*-transferase Yc subunit	K01932_f_at	1.78	−0.88
Glutathione *S*-transferase Ycl subunit	S72505_f_at	1.73	−0.87
UDP glucuronosyltransferase-21 (UDPGTr-21)	M33747_at	1.50	−0.85
UDP-glucuronosyltransferase, phenobarbital-inducible	M13506_at	1.88	−0.84
Sulfotransferase K2[a]	rc_AI638982_at	1.15	−0.83
UDP glucuronosyltransferase-5 (UDPGTr-5)	M33746mRNA#2_f_at	1.37	−0.81
Hydrolysis			
GTP cyclohydrolase 1	E03424cds_s_at	1.64	−0.97
Epoxide hydrolase	M26125_at	2.22	−0.96
Carboxylesterase	M20629_s_at	1.51	−0.95
Carboxyesterase E1	D00362_s_at	1.54	−0.81
Reduction			
Aldo-keto reductase family 7, member A2[a]	rc_AA892821_at	1.20	−0.92
Aflatoxin B1 aldehyde reductase (AFAR)	AF045464_s_at	9.36	−0.91
Glutathione reductase	U73174_at	1.69	−0.87
NAD(P)H-menadione oxidoreductase	J02679_s_at	2.10	−0.85
Glutathione synthesis			
Gamma-glutamylcysteine synthetase	J05181_at	2.61	−0.94
Gultamate-cystein ligase, modifier subunit (Gclm)[a]	rc_AI233261_i_at	2.23	−0.91
Gamma-glutamylcysteine synthetase light chain	S65555_g_at	2.70	−0.87
Antioxidant			
Metallothionein-2 and Metallothionein-1	M11794cds#2_f_at	13.78	−0.93
Ferritin light chain 2 (Ft12)[a]	rc_AI231807_at	1.64	−0.90
Ferritin light chain 2 (Ft12)[a]	rc_AI231807_g_at	1.67	−0.89
Thiol-specific antioxidant protein (1-Cys peroxiredoxin)	Y17295cds_s_at	1.28	−0.85
Lipid metabolism			
Carnitine palmitoyltransferase I	L07736_at	2.20	−0.98
Delta-4-3-ketosteroid 5-beta-reductase	D17309_at	1.73	−0.96
Putative peroxisomal 2,4-dienoyl-CoA reductase	AF044574_at	1.22	−0.94
Delta-4-3-ketosteroid 5-beta-reductase	S80431_s_at	1.96	−0.93
2,4-Dienoyl-CoA reductase	D00569_at	1.65	−0.91
Acyl-coA oxidase	J02752_at	1.27	−0.89
Fatty acid Coenzyme A ligase, long chain 4[a]	rc_AI236284_s_at	1.65	−0.89
Long-chain enoyl-CoA hydratase/3-hydroxyacyl-	D16478_at	1.15	−0.89
HMG-CoA reductase	X55286_g_at	1.91	−0.81
3-Hydroxy-3-memylg1utaryl coenzyme A reductase	M29249eds_at	2.17	−0.81
Transcription factor			
Small heterodimer partner homologue	D86745exon_s_at	3.10	−0.90
Small heterodimer partner homologue	D86745exon_s_at	2.59	−0.90
Small heterodimer partner homologue	D86580_at	2.52	−0.88
Hepatocyte nuclear factor 4 (HNF4)	X57133mRNA_at	1.35	−0.86
Signal transduction			
Cyclin-dependent kinase 4 (cdk4)	L11007_at	1.38	−0.91
S6 kinase	M57428_s_at	1.30	−0.82
Protein kinase C regulatory protein	S55305_s_at	1.43	−0.81
A-kinase anchor protein121	AF068202_at	1.17	−0.80
Miscellaneous			
Sodium-dependent multi-vitamin transporter	AF026554_at	1.34	−0.94
Polypyrimidine tract binding protein	X74565cds_g_at	1.36	−0.92
Microtubule-associated proteins 1A and 1B light chain 3 subunit	U05784_s_at	1.27	−0.92

Table 2 (*Continued*)

Annotation	Affymetrix ID	Fold change	Pearson's *r*
Caspase 6 (Mch2)	AF025670_g_at	1.50	−0.90
Cytochrome P450 arachidonic acid epoxygenase (cyp2C23)	U04733_s_at	1.22	−0.89
Differentiation antigen CD14	AF087944mRNA_s_at	1.44	−0.89
GABA transporter GAT-2	M95762 at	1.46	−0.86
Tricarboxylate carrier	S70011_g_at	1.42	−0.85
Hereditary haemochromatosis-like protein	AJ001517cds_at	1.38	−0.85
Kallikrein	M30282_at	1.21	−0.85
Keratin complex 1[a]	rc_AI072634_at	1.40	−0.84
Amyloid precursor-like protein 2	X77934cds_at	1.24	−0.84
ATPase inhibitor protein	D13122_f_at	1.65	−0.84
RNA binding protein gene with multiple splicing[a]	rc_AA859519_g_at	1.26	−0.84
Ribosomal protein S6	M29358_g_at	1.16	−0.83
CD14	AF087943_s_at	1.43	−0.83
Type I thyroxine deiodinase	X57999cds_at	1.23	−0.82
Adaptor-related protein complex 2, mu 1 subunit[a]	rc_AI012807_at	1.19	−0.82
Retinol dehydrogenase type II	U33500_g_at	1.23	−0.81
TRPM-2	M64733mRNA_s_at	1.21	−0.81
Malic enzyme (MAL)[a]	rc_AI171506_at	1.91	−0.81

Glutathione deficiency-correlated probe sets were determined by selecting genes that showed statistically significant differences (Spearman's correlation, $P < 0.05$) and a Pearson's r less than −0.8 between the hepatic mRNA level and hepatic glutathione content. The highlighted gene probes also represent BSO-specific genes. Fold change: fold changes calculated by dividing the mean transcription level of chemical-treated rats ($n = 4$) with that of the control ($n = 4$). Pearson's *r*: Pearson's r between the mRNA level and glutathione content.

[a] Annotated gene probes by BLAST Homology Search.

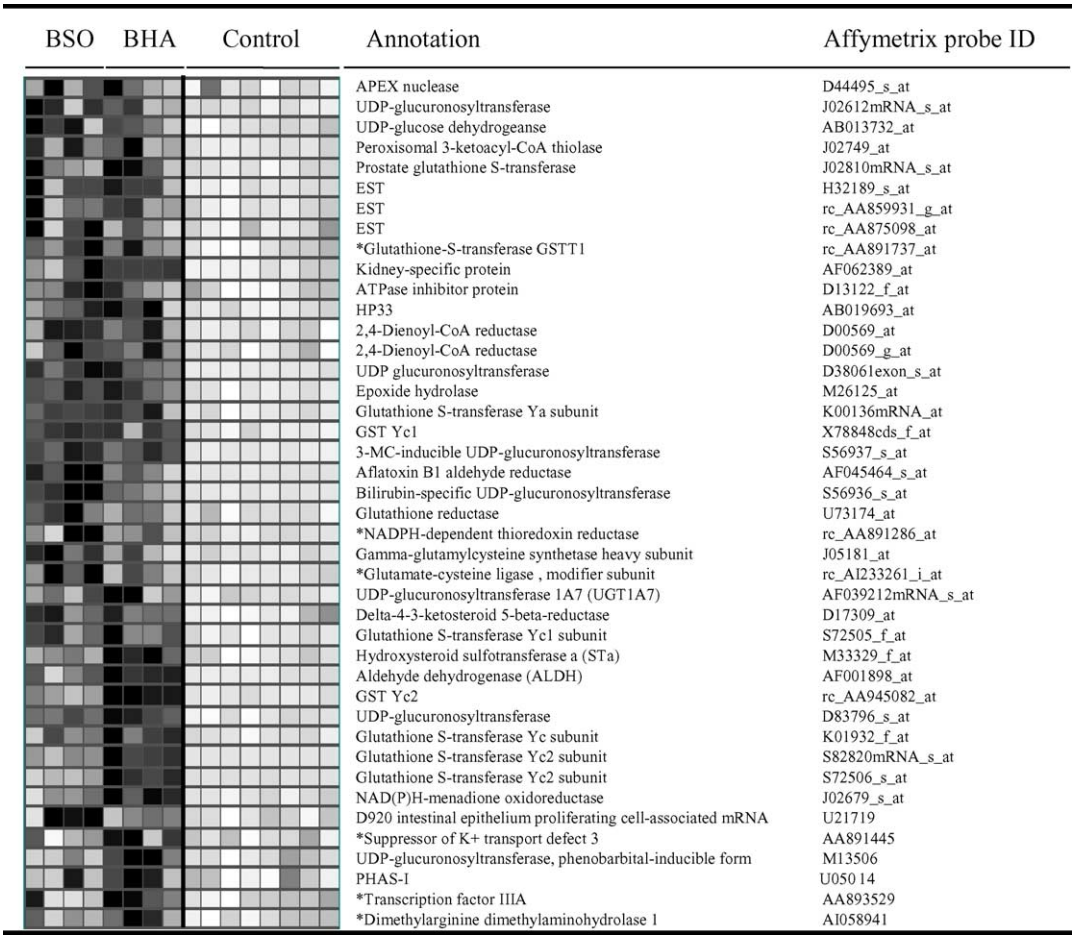

Fig. 3. Dually-induced genes. Genes that showed an increase in mRNA contents after the BSO and BHA treatments were identified as dually-induced gene probes. The colors of the heat map represent the mRNA content levels: white for low, gray for intermediate, and black for high transcription levels. *Annotated gene probes by BLAST Homology Search.

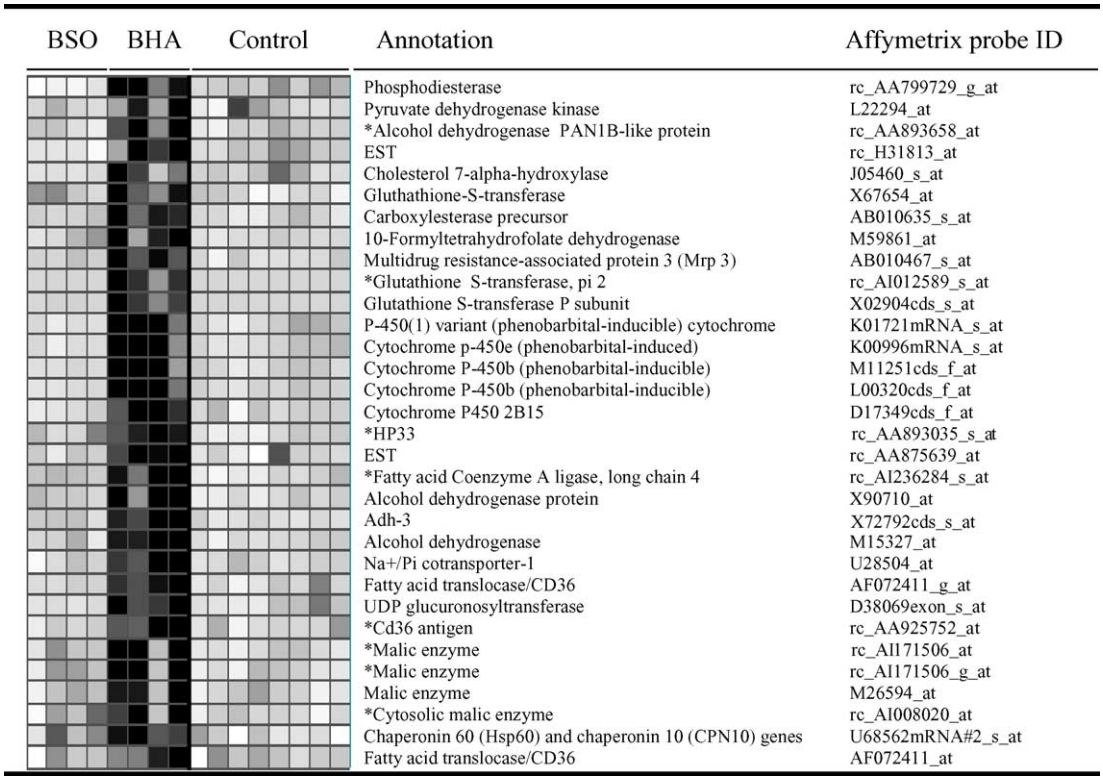

Fig. 4. BHA-specific induced genes. Genes, which showed mRNA contents that increased specifically by the BHA-treatment, were determined as BHA-specific gene probes. The colors of the heat map represent the mRNA content levels: white for low, gray for intermediate, and black for high transcription levels. * Annotated gene probes by BLAST Homology Search.

utilization, were identified in the BSO-specific gene probes.

3.4. Real-time quantitative RT-PCR analysis for BSO-specific genes

The hepatic mRNA contents of six BSO-specific genes namely: γ-GCS, glutathione reductase I, ferritin light-chain 2 and GTP cyclohydrolase I, were measured by quantitative RT-PCR (Fig. 6). The hepatic mRNA contents of the γ-GCS, glutathione reductase I, ferritin light-chain 2 and GTP cyclohydrolase I, were significantly increased after the BSO treatment ($P < 0.05$) by average fold-inductions of 4.3, 2.5, 2.0 and 1.8, respectively. The hepatic mRNA contents of all the investigated genes were not significantly changed by the BHA treatment.

3.5. Principal component analysis

The PCA results showed characteristic gene expression profiles in rat livers treated with BSO, BHA, APAP, PB or CLO. The difference in gene expression profiles between APAP-treated and control rat livers increased with time, and the gene expression profile 24 h after the APAP treatment became close to that of the BSO-treated rats (Fig. 7). The gene expression profile of PB-treated rats on day 1 was close to that of the BHA-treated rats, and the gene expression time profiles differed after repetitive PB treatments. The gene expression profile of CLO-treated rats was similar to that of the control irrespective of the dosing frequency.

4. Discussion

In the present study, we identified 69 glutathione deficiency-correlated genes (referred to as ‘‘glutathione-deficiency genes’’) probes by using BSO-treated rats as a glutathione deficient animal model. The hepatic glutathione content of these rats was approximately 0.19-fold that of the control. Of all the genes on the RG U34 GeneChip microarray, the GST Ya subunit gene exhibited an expression profile that was most inversely-correlated to that of the hepatic glutathione content. GST Ya is the first gene recognized to have an ARE element in the promoter, and is regulated by the transcription factor Nrf2 [16,28]. Other than GST Ya, many of the glutathione-deficiency genes were reported to be controlled by Nrf2 in mice, such as the genes involved in the conjugation of reactive electrophilic compounds (GST Yc1, Yc2 and UDPGT 2 family genes), hydrolysis (epoxide hydrolase and carboxylesterase), reduction (aldo-keto reductase and glutathione reductase I), glutathione synthesis (γ-GCS) and antioxidation (metallothionein and ferritin) [29,30]. These results demonstrate the validity of our method for identifying glutathione-deficiency genes.

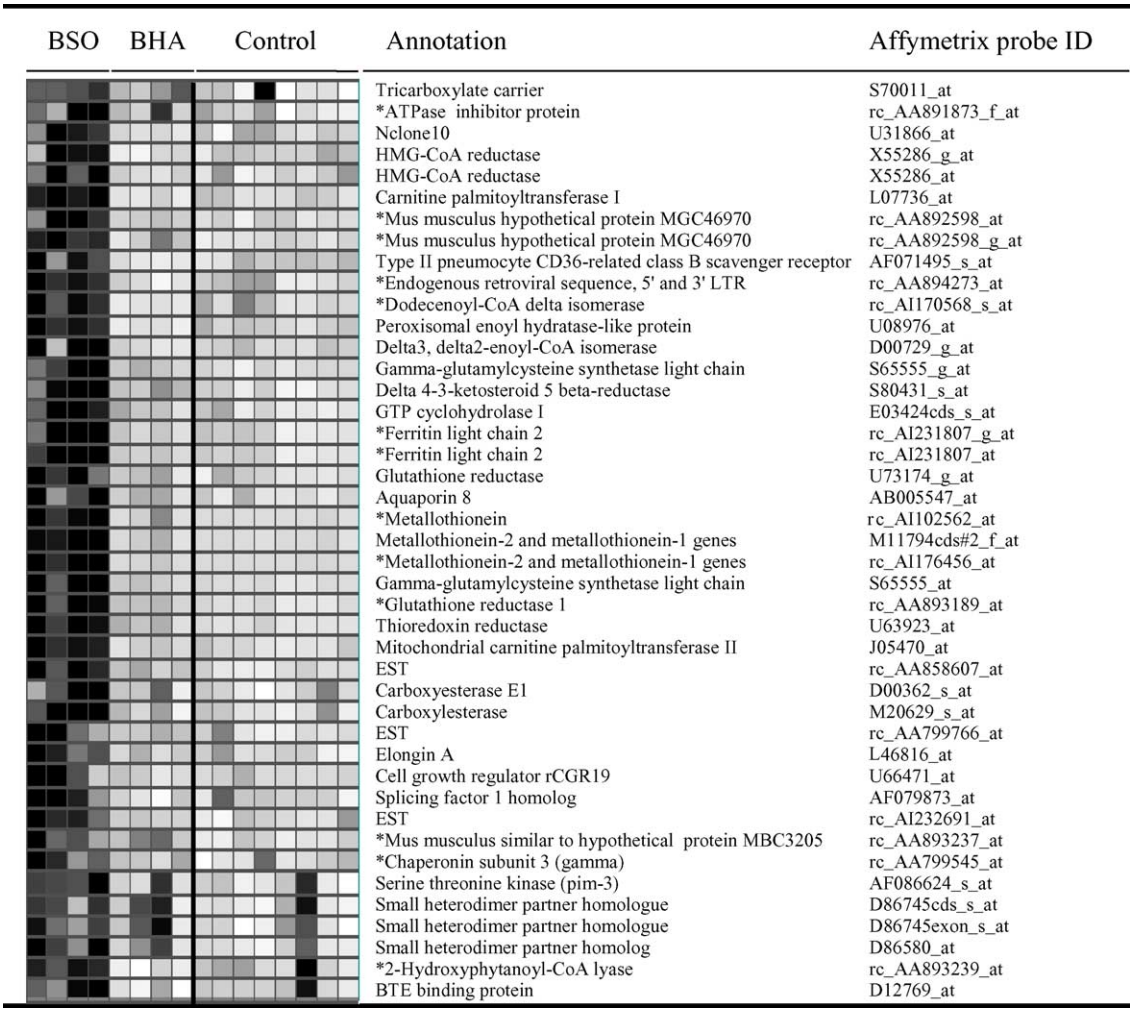

BSO	BHA	Control	Annotation	Affymetrix probe ID
			Tricarboxylate carrier	S70011_at
			*ATPase inhibitor protein	rc_AA891873_f_at
			Nclone10	U31866_at
			HMG-CoA reductase	X55286_g_at
			HMG-CoA reductase	X55286_at
			Carnitine palmitoyltransferase I	L07736_at
			*Mus musculus hypothetical protein MGC46970	rc_AA892598_at
			*Mus musculus hypothetical protein MGC46970	rc_AA892598_g_at
			Type II pneumocyte CD36-related class B scavenger receptor	AF071495_s_at
			*Endogenous retroviral sequence, 5' and 3' LTR	rc_AA894273_at
			*Dodecenoyl-CoA delta isomerase	rc_AI170568_s_at
			Peroxisomal enoyl hydratase-like protein	U08976_at
			Delta3, delta2-enoyl-CoA isomerase	D00729_g_at
			Gamma-glutamylcysteine synthetase light chain	S65555_g_at
			Delta 4-3-ketosteroid 5 beta-reductase	S80431_s_at
			GTP cyclohydrolase I	E03424cds_s_at
			*Ferritin light chain 2	rc_AI231807_g_at
			*Ferritin light chain 2	rc_AI231807_at
			Glutathione reductase	U73174_g_at
			Aquaporin 8	AB005547_at
			*Metallothionein	rc_AI102562_at
			Metallothionein-2 and metallothionein-1 genes	M11794cds#2_f_at
			*Metallothionein-2 and metallothionein-1 genes	rc_AI176456_at
			Gamma-glutamylcysteine synthetase light chain	S65555_at
			*Glutathione reductase 1	rc_AA893189_at
			Thioredoxin reductase	U63923_at
			Mitochondrial carnitine palmitoyltransferase II	J05470_at
			EST	rc_AA858607_at
			Carboxyesterase E1	D00362_s_at
			Carboxylesterase	M20629_s_at
			EST	rc_AA799766_at
			Elongin A	L46816_at
			Cell growth regulator rCGR19	U66471_at
			Splicing factor 1 homolog	AF079873_at
			EST	rc_AI232691_at
			*Mus musculus similar to hypothetical protein MBC3205	rc_AA893237_at
			*Chaperonin subunit 3 (gamma)	rc_AA799545_at
			Serine threonine kinase (pim-3)	AF086624_s_at
			Small heterodimer partner homologue	D86745cds_s_at
			Small heterodimer partner homologue	D86745exon_s_at
			Small heterodimer partner homolog	D86580_at
			*2-Hydroxyphytanoyl-CoA lyase	rc_AA893239_at
			BTE binding protein	D12769_at

Fig. 5. BSO-specific induced genes. Genes, which showed mRNA contents that increased specifically by the BSO-treatment, were determined as BSO-specific gene probes. The colors of the heat map represent the mRNA content levels: white for low, gray for intermediate, and black for high transcription levels. * Annotated gene probes by BLAST Homology Search.

PCA was performed using the glutathione-deficiency gene probes to narrow the range of gene expression data [31], and the results demonstrated that the glutathione-deficiency gene probes could classify the gene expression profiles according to hepatic glutathione levels. For example, the post dose hepatic gene expression profiles of APAP-treated rats differed increasingly with time from the profile of the controls, suggesting time-related hepatocellular glutathione depletion in the APAP-treated rat livers. In the PCA results, the gene expression profiles of APAP-treated rats 24 h after the dosing, were close to those of BSO-treated rats, indicating that APAP treatment depleted cellular glutathione at 24 h after the dosing at the close to those of BSO-treated rat livers. The PCA results indicated that the CLO treatment did not strongly affect the expression profiles of the glutathione-deficiency genes. It was reported that CLO causes oxidative stress via an induction of peroxisomal oxidation enzymes but increases the cellular glutathione level [32–34]. The reason why the CLO treatment did not affect the expression of the glutathione-deficiency genes is not clear, but one possibility is that the level of oxidation and glutathione availability, which may have been affected by the CLO treatment, counterbalanced the hepatic redox balance, or hepatic glutathione balance. The gene expression profile of the PB-treated rats gradually changed with time, and became similar to that of the BHA-treated rats. Repeated PB treatment is reported to increase the hepatic glutathione content [35], and therefore the PCA result was thought to be reasonable. Overall, the PCA results using the BSO-deficiency probes were reasonable considering the previous reports, and thus, the glutathione-deficiency gene probes identified in the present study are considered to be useful for the evaluation of hepatic glutathione level after the chemical treatment.

One of the problems foreseen in utilizing the glutathione-deficiency gene probes identified in the study, however, is the presence of a number of Nrf2-regulated phase II DME and antioxidants in the probe set, because there are compounds that stimulate the Nrf2 signal without

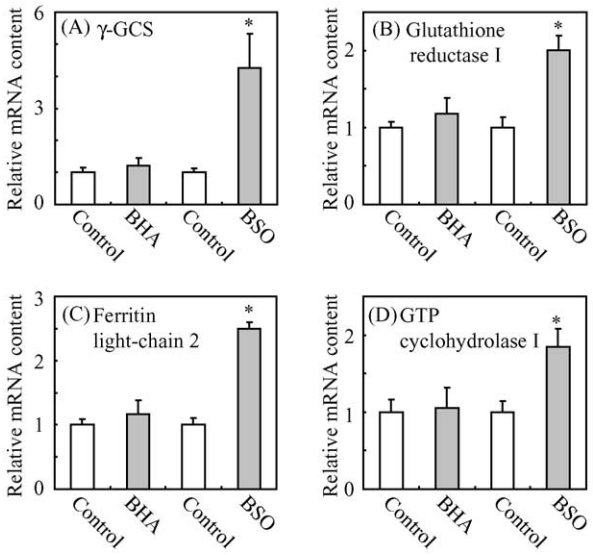

Fig. 6. Real-time quantitative RT-PCR results. Real-time quantitative RT-PCR was conducted on rat livers treated with BSO or BHA. (A) γ-GCS (accession no. S65555), (B) glutathione reductase I (U73174), (C) ferritin light-chain 2 (AI231807), and (D) GTP cyclohydrolase I (E03424). * Significantly different from the control group ($P < 0.01$).

oxidative stress such as BHA [21]. To gain further information for discerning the genes up-regulated only by oxidative stress from the microarray data, we next compared the gene expression profile of BSO-treated rat liver with that of BHA-treated rat livers, and identified three mRNA induction patterns: BSO-specific, BHA-specific and dually-induced genes. In addition to the induction of various phase II DME genes by the BHA treatment as reported previously [21,36], the mRNA contents of CAR-regulated genes such as *CYP2B*, Mrp3 and aldehyde dehydrogenase were also increased [37,38], indicating that a part of the increase in mRNA contents of phase II DME genes after the BHA treatment was brought about by a stimulation of the nuclear receptor CAR. The similar expression profiles of some glutathione-deficient genes in rat livers after PB and BHA treatment as determined by PCA analysis reflect the CAR stimulation effect of both chemicals. Based on this result, when we evaluate the hepatic glutathione status using the glutathione-deficiency gene probes, we must consider the effect of receptor-mediated pathways [9], since many of the phase II DME gene expressions are regulated not only by the transcription factor Nrf2 but also by the nuclear receptors such as CAR, PXR and AhR [9]. The stimulation of nuclear receptors could be assessed by observing the clustered changes in the mRNA contents of target genes such as phase I DME genes [36], which would also lead to a more comprehensive gene expression analysis.

Since the BSO treatment did not affect the content of any phase I DME mRNA, the induction of phase II DME and antioxidant genes were thought to be induced exclusively due to glutathione deficiency and the following oxidative stress. Therefore, genes induced specifically by BSO, such as GTP cyclohydrolase I, ferritin light-chain 2, metallothionein and glutathione reductase I, would be suitable indicators of glutathione deficiency. Of these 14 BSO-specific gene probes, the microarray results of the four representative genes namely: γ-GCS, glutathione reductase I, ferritin light-chain 2 and GTP cyclohydrolase I, were confirmed by real-time quantitative RT-PCR analysis.

GTP cyclohydrolase I is a rate-limiting enzyme in the tetrahydrobiopterin pathway [39,40]. Since tetrahydrobiopterin was reported to have antioxidative activity in pheochromocytoma PC 12 cells in the presence of peroxidase and NADH [41], the increase in the mRNA content of

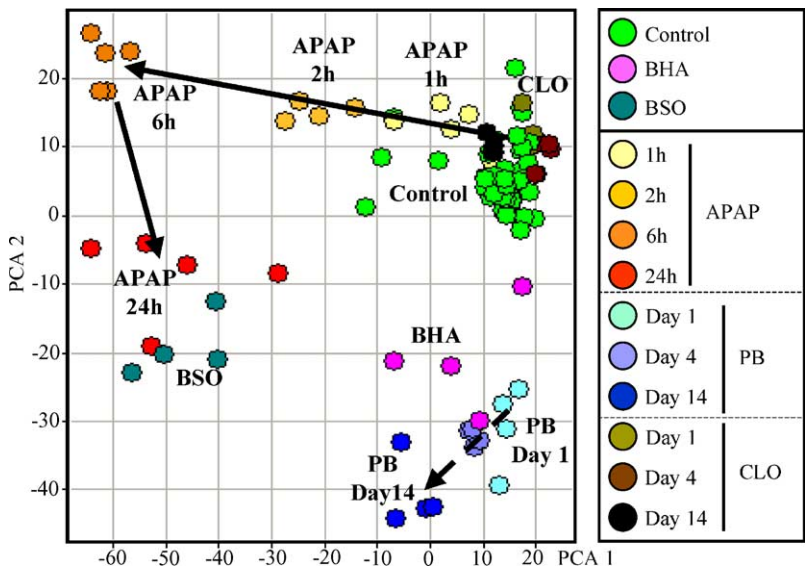

Fig. 7. Principal component analysis. Principal component analysis of gene expression profiles of BSO, BHA, APAP, PB- or CLO-treated rat livers at various time points. Each spot represents the gene expression profile of individual rats. Solid and dashed arrows represent the time-course of changes in gene expression profiles of rat livers treated with APAP or PB, respectively.

GTP cyclohydrolase I was suggested to be due to the oxidative condition of the BSO-treated rat livers. Ferritin is a 24-subunit protein composed of heavy and light chains, and is reported to protect cells against oxygen free radical-mediated damage [42,43]. In mice, putative ARE sequences were identified in both ferritin heavy and light chains [44]. Metallothionein, a scavenger of hydroxyl radicals, protected DNA from the oxidative attack by microsomes [45]. It was suggested that metallothionein had a protective effect against glutathione depletion in rat hepatocytes [46]. Much higher metallothionein mRNA content was observed in the BSO-treated rat livers, suggesting cellular oxidative stress as well. Glutahione reductase I converts the oxidated form of glutathione to the reduced form [3]. Therefore, the strong induction of glutathione reductase I in the BSO-treated rat livers suggested a stimulated redox cycle due to the glutathione deficiency. Thus, a clustered increase in the mRNA contents of these BSO-specific genes would be a suitable marker to appropriately evaluate the extent of cellular glutathione deficiency based on the microarray data.

In conclusion, we identified glutathione deficiency-correlated marker genes, which are useful for the evaluation of the cellular glutathione level based on microarray data by PCA analysis. In utilizing the marker genes, however, nuclear receptor-mediated effects should be considered by observing the expression changes of their target genes. In addition, the expression levels of BSO-specific genes identified in the present study would provide useful information for evaluating glutathione deficiency. This analytical procedure would be helpful for the safety evaluation of pharmaceuticals under development in terms of the potential risk of APAP-type hepatic injury, in preclinical studies.

References

[1] Lee WM. Drug-induced hepatotoxicity. N Engl J Med 2003;349:474–85.

[2] Hentze H, Latta M, Kunstle G, Lucas R, Wendel A. Redox control of hepatic cell death. Toxicol Lett 2003;139:111–8.

[3] Lu SC. Regulation of hepatic glutathione synthesis: current concepts and controversies. FASEB J 1999;13:1169–83.

[4] Raza H, Robin MA, Fang JK, Avadhani NG. Multiple isoforms of mitochondrial glutathione *S*-transferases and their differential induction under oxidative stress. Biochem J 2002;366:45–55.

[5] Dahlin DC, Miwa GT, Lu AY, Nelson SD. *N*-acetyl-*p*-benzoquinone imine: a cytochrome P-450-mediated oxidation product of acetaminophen. Proc Natl Acad Sci USA 1984;81:1327–31.

[6] James LP, Mayeux PR, Hinson JA. Acetaminophen-induced hepatotoxicity. Drug Metab Dispos 2003;31:1499–506.

[7] Mitchell JR, Jollow DJ, Potter WZ, Gillette JR, Brodie BB. Acetaminophen-induced hepatic necrosis. IV. Protective role of glutathione. J Pharmacol Exp Ther 1973;187:211–7.

[8] Parkinson A. Biotransformation of xenobiotics. In: Klaassen CD, editor, Casarett and Doull's toxicology, New York: McGraw-Hill; 2001. pp. 133–224.

[9] Rushmore TH, Kong AN. Pharmacogenomics, regulation and signaling pathways of phase I and II drug metabolizing enzymes. Curr Drug Metab 2002;3:481–90.

[10] Honkakoski P, Negishi M. Regulatory DNA elements of phenobarbital-responsive cytochrome P450 CYP2B genes. J Biochem Mol Toxicol 1998;12:3–9.

[11] Rowlands JC, Gustafsson JA. Aryl hydrocarbon receptor-mediated signal transduction. Crit Rev Toxicol 1997;27:109–34.

[12] Nguyen T, Huang HC, Pickett CB. Transcriptional regulation of the antioxidant response element. Activation by Nrf2 and repression by MafK. J Biol Chem 2000;275:15466–73.

[13] Itoh K, Chiba T, Takahashi S, Ishii T, Igarashi K, Katoh Y, et al. An Nrf2/small Maf heterodimer mediates the induction of phase II detoxifying enzyme genes through antioxidant response elements. Biochem Biophys Res Commun 1997;236:313–22.

[14] McMahon M, Itoh K, Yamamoto M, Chanas SA, Henderson CJ, McLellan LI, et al. The Cap'n'Collar basic leucine zipper transcription factor Nrf2 (NF-E2 p45-related factor 2) controls both constitutive and inducible expression of intestinal detoxification and glutathione biosynthetic enzymes. Cancer Res 2001;61:3299–307.

[15] Dhakshinamoorthy S, Jaiswal AK. Functional characterization and role of INrf2 in antioxidant response element-mediated expression and antioxidant induction of NAD(P)H:quinone oxidoreductase1 gene. Oncogene 2001;20:3906–17.

[16] Rushmore TH, Pickett CB. Transcriptional regulation of the rat glutathione S-transferase Ya subunit gene. Characterization of a xenobiotic-responsive element controlling inducible expression by phenolic antioxidants. J Biol Chem 1990;265:14648–53.

[17] Alam J, Stewart D, Touchard C, Boinapally S, Choi AM, Cook JL. Nrf2, a Cap'n'Collar transcription factor, regulates induction of the heme oxygenase-1 gene. J Biol Chem 1999;274:26071–8.

[18] Moinova HR, Mulcahy RT. Up-regulation of the human gamma-glutamylcysteine synthetase regulatory subunit gene involves binding of Nrf2 to an electrophile responsive element. Biochem Biophys Res Commun 1999;261:661–8.

[19] Griffith OW, Meister A. Potent and specific inhibition of glutathione synthesis by buthionine sulfoximine (S-*n*-butyl homocysteine sulfoximine). J Biol Chem 1979;254:7558–60.

[20] Watanabe T, Sagisaka H, Arakawa S, Shibaya Y, Watanabe M, Igarashi I, et al. A novel model of continuous depletion of glutathione in mice treated with L-buthionine (*S, R*)-sulfoximine. J Toxicol Sci 2003;28:455–69.

[21] Hayes JD, Chanas SA, Henderson CJ, McMahon M, Sun C, Moffat GJ, et al. The Nrf2 transcription factor contributes both to the basal expression of glutathione *S*-transferases in mouse liver and to their induction by the chemopreventive synthetic antioxidants, butylated hydroxyanisole and ethoxyquin. Biochem Soc Trans 2000;28:33–41.

[22] Yang MC, Ruan QG, Yang JJ, Eckenrode S, Wu S, McIndoe RA, et al. A statistical method for flagging weak spots improves normalization and ratio estimates in microarrays. Physiol Genomics 2001;7:45–53.

[23] Rabow AA, Shoemaker RH, Sausville EA, Covell DG. Mining the National Cancer Institute's tumor-screening database: identification of compounds with similar cellular activities. J Med Chem 2002;45:818–40.

[24] Kasturi J, Acharya R, Ramanathan M. An information theoretic approach for analyzing temporal patterns of gene expression. Bioinformatics 2003;19:449–58.

[25] Urbanczyk-Wochniak E, Luedemann A, Kopka J, Selbig J, Roessner-Tunali U, Willmitzer L, et al. Parallel analysis of transcript and metabolic profiles: a new approach in systems biology. EMBO Rep 2003;4:989–93.

[26] Altschul SF, Madden TL, Schaffer AA, Zhang J, Zhang Z, Miller W, et al. Gapped BLAST and PSI-BLAST: a new generation of protein database search programs. Nucleic Acids Res 1997;25:3389–402.

[27] Draghici S, Cluster analysis. In: Etheridge AM, Gross LJ, Lenhart S, Maini PK, Safer HM, Voit EO, editors. Data analysis tools for DNA microarrays. London: CRC Press; 2003. pp. 263–307.
[28] Rushmore TH, Morton MR, Pickett CB. The antioxidant responsive element. Activation by oxidative stress and identification of the DNA consensus sequence required for functional activity. J Biol Chem 1991;266:11632–9.
[29] Lee JM, Calkins MJ, Chan K, Kan YW, Johnson JA. Identification of the NF-E2-related factor-2-dependent genes conferring protection against oxidative stress in primary cortical astrocytes using oligonucleotide microarray analysis. J Biol Chem 2003;278:12029–38.
[30] Thimmulappa RK, Mai KH, Srisuma S, Kensler TW, Yamamoto M, Biswal S. Identification of Nrf2-regulated genes induced by the chemopreventive agent sulforaphane by oligonucleotide microarray. Cancer Res 2002;62:5196–203.
[31] Heijne WH, Stierum RH, Slijper M, van Bladeren PJ, van Ommen B. Toxicogenomics of bromobenzene hepatotoxicity: a combined transcriptomics and proteomics approach. Biochem Pharmacol 2003;65:857–75.
[32] Chen C, Hennig GE, Whiteley HE, Corton JC, Manautou JE. Peroxisome proliferator-activated receptor alpha-null mice lack resistance to acetaminophen hepatotoxicity following clofibrate exposure. Toxicol Sci 2000;57:338–44.
[33] Mehendale HM. PPAR-alpha: a key to the mechanism of hepatoprotection by clofibrate. Toxicol Sci 2000;57:187–90.
[34] Gonzalez FJ, Peters JM, Cattley RC. Mechanism of action of the nongenotoxic peroxisome proliferators: role of the peroxisome proliferator-activator receptor alpha. J Natl Cancer Inst 1998;90:1702–9.
[35] Videla LA, Arisi AC, Fuzaro AP, Koch OR, Junqueira VB. Prolonged phenobarbital pretreatment abolishes the early oxidative stress component induced in the liver by acute lindane intoxication. Toxicol Lett 2000;115:45–51.
[36] Kiyosawa N, Watanabe T, Sakuma K, Kanbori M, Niino N, Ito K, et al. Phylogenetic tree facilitates the understanding of gene expression data on drug metabolizing enzymes obtained by microarray analysis. Toxicol Lett 2003;145:281–9.
[37] Xiong H, Yoshinari K, Brouwer KL, Negishi M. Role of constitutive androstane receptor in the in vivo induction of Mrp3 and CYP2B1/2 by phenobarbital. Drug Metab Dispos 2002;30:918–23.
[38] Ganem LG, Jefcoate CR. Endocrine factors modulate the phenobarbital-mediated induction of cytochromes P450 and phase II enzymes in a similar strain-dependent manner. Toxicol Appl Pharmacol 1998;150:68–75.
[39] Geller DA, Di Silvio M, Billiar TR, Hatakeyama K. GTP cyclohydrolase I is coinduced in hepatocytes stimulated to produce nitric oxide. Biochem Biophys Res Commun 2000;276:633–41.
[40] Nichol CA, Smith GK, Duch DS. Biosynthesis and metabolism of tetrahydrobiopterin and molybdopterin. Annu Rev Biochem 1985;54:729–64.
[41] Shen RS, Zhang YX. Antioxidation activity of tetrahydrobiopterin in pheochromocytoma PC 12 cells. Chem Biol Interact 1991;78:307–19.
[42] Orino K, Lehman L, Tsuji Y, Ayaki H, Torti SV, Torti FM. Ferritin and the response to oxidative stress. Biochem J 2001;357:241–7.
[43] Arosio P, Levi S. Ferritin, iron homeostasis. Free Radic Biol Med 2002;33:457–63.
[44] Tsuji Y, Ayaki H, Whitman SP, Morrow CS, Torti SV, Torti FM. Coordinate transcriptional and translational regulation of ferritin in response to oxidative stress. Mol Cell Biol 2000;20:5818–27.
[45] Miura T, Muraoka S, Ogiso T. Antioxidant activity of metallothionein compared with reduced glutathione. Life Sci 1997;60:301–9.
[46] Haidara K, Moffatt P, Denizeau F. Metallothionein induction attenuates the effects of glutathione depletors in rat hepatocytes. Toxicol Sci 1999;49:297–305.